Доклади на Българската академия на науките
Comptes rendus de l'Académie bulgare des Sciences
Tome 77, No 1, 2024

CHEMISTRY
Inorganic chemistry

UPCONVERSION LUMINESCENCE PROPERTIES OF $Ho^{3+}/Tm^{3+}/Yb^{3+}$ CO-DOPED $NaGd(MO_4)_2$ PREPARED BY HYDROTHERMAL METHOD

Zhaoguang Zhang✉, Kuaile Dang, Huajian Li, Zeyu Song, Xiaochen Yu

Received on July 19, 2023
Presented by V. Bankova, Corresponding Member of BAS, on November 28, 2023

Abstract

In this paper, $Ho^{3+}/Tm^{3+}/Yb^{3+}$-doped $NaGd(MO_4)_2$ phosphors were prepared using the hydrothermal method and the effect of Yb^{3+} doping amount on the luminescence properties of these phosphor materials was investigated. $NaGd(MO_4)_2$ was characterized using X-ray diffraction (XRD), scanning electron microscopy (SEM), and spectral analysis. The results showed that $Ho^{3+}/Tm^{3+}/Yb^{3+}$-doped $NaGd(MO_4)_2$ has tetragonal phase structures, and doping with rare-earth ions decreases the cell parameters of $NaGd(MO_4)_2$. $NaGd(MO_4)_2$:$Ho^3/Tm^{3+}/Yb^{3+}$ generates blue, green, and red lights at 477, 545, and 659 nm, respectively, under an excitation of 980 nm. The emission of these three lights is called a three-photon process. As the doping ratio of Yb^{3+} increases, the colour coordinates of samples gradually approach the white region from the red region, enabling $NaGd(MO_4)_2$:0.1Ho/1Tm/20Yb to exhibit white emission. Doping with Yb^{3+} increases the energy transfer and quantum efficiencies of $NaGd(MO_4)_2$. When the concentration of Yb^{3+} reached 30%, the quantum efficiency of $NaGd(MO_4)_2$ reached the maximum value of 188.37%. Overall, $NaGd(MO_4)_2$:Ho/Tm/Yb has broad application prospects in the field of white lighting.

Key words: rare-earth doping, $NaGd(MO_4)_2$, white light, fluorescence lifetime, emission spectrum

This study was supported by the China Postdoctoral Science Foundation (2019M602145), the National Natural Science Foundation of China (51102023), and the Central Universities Basic Research Operation Fund (CHD300102310501).

https://doi.org/10.7546/CRABS.2024.01.02

Introduction. Rare-earth (RE) elements include lanthanum (La), cerium (Ce), praseodymium (Pr), and 17 other lanthanide metal elements, and their rich electronic energy levels endow them with diverse fluorescence properties [1]. The advantages of RE luminescent materials include stable physical and chemical properties, high conversion efficiency, and strong absorption ability [2]. The luminescence exhibited by these materials can be classified into upconversion (UC) luminescence and quantum cutting (QC). The UC luminescence materials are excited by low-energy light and emits high-energy light, i.e., they are excited by long-wavelength and low-frequency light and emit short-wavelength and high-frequency light [3]. White light emission is widely used due to its high life, high energy efficiency, and excellent stability, especially in lighting and image display. UC white light is generated by converting high-energy light into low-energy light. The common method used for this purpose is to achieve spectral superposition by combining different RE elements and their relative content, thereby producing white light emission. RE elements are prone to lose three electrons from their 5d, 6s, and 4f orbitals, but the 4f electrons are shielded by the $5s^2 5p^6$ shell layer and usually behave as +3 valence ions [4]. Various studies have been conducted on the Er^{3+}–Tm^{3+} and Ho^{3+}–Yb^{3+}systems and adjusting the doping concentration and type of RE element to demonstrate UC and QC processes [5–7].

In recent years, RE-doped white light materials have become a research focus in the field of lighting [8]. RE ion Eu^{2+}-doped $12CaO{\cdot}7Al_2O_3$(C12A7) can exhibit strong blue emission at 477 nm [9]. By mixing Gd^{3+} with $NaYF_4$:Yb:Er nanoparticles, red and green lights with different intensities can be obtained by controlling the doping ratio of Gd^{3+}, confirming that it is possible to prepare composites of white light materials by controlling the proportion of RE elements [10]. The selection of matrix materials directly affects the performance of luminescent materials. Molybdate has a unique tetragonal structure and low phonon energy and is often used as an excellent matrix for UC luminescence materials [11]. Shi et al. [12] synthesized $Nd^{3+}/Yb^{3+}/Tm^{3+}$ co-doped $NaY(WO_4)_2$ nanocrystals using the hydrothermal method and analyzed their UC luminescence properties with the 808 nm excitation light. They found that the blue light of $NaY(WO_4)_2$, which appeared at 469 nm, could be attributed to the transition of $Tm^{3+}$from $^1G_4$ energy level to $^3H_6$ energy level, the green light at 539 nm was attributed to the transition of of $Tm^{3+}$from the $^1D_2$ energy level to Tm^{3+} to $^3H_5$. In recent years, many studies have investigated the triple doping of RE elements [13]. Because the emission spectra of Ho^{3+} and Tm^{3+} are superimposed on each other, a continuous spectrum is formed, covering the entire visible region. Yb^{3+} has an abundant electron energy level structure and multiple excited energy levels, enabling the effective absorption of high-energy photons and transfer the absorbed energy to Ho^{3+} and Tm^{3+} through nonradiative energy transfer. The adjustment of Yb^{3+} doping ratio affects the efficiency of the entire energy transfer process and shape and width of the emission spectrum. Moreover, adjusting the Yb^{3+}

ratio can optimize the overall optical emission system.

This paper aims to obtain white light materials with long life and high conversion efficiency and promote the innovation of RE elements in the field of illumination luminescence. In this paper, molybdate with stable physical and chemical properties is used as the matrix material, the ratio of Ho^{3+}/Tm^{3+} is fixed, the ratio of Yb^{3+} is adjusted, and the UC luminescence performance and quantum shear of $NaGd(MO_4)_2$ are improved. While realizing white light emission, this paper also lays a research foundation for the development of white light materials with excellent performance.

Experimental. ***Materials.*** RE oxides Gd_2O_3 (99.99%), Ho_2O_3 (99.99%), and Yb_2O_3 (99.99%) (all industrial grade) were purchased from Ganzhou Rare Friends New Materials Co., Ltd. Reagents were purchased from Jiangxi Province, China. $Na_2MoO_4{\cdot}2H_2O$ (99.5%), nitric acid (99.5%), and oleic acid (99.5%) were purchased from Sinopharm Chemical Reagent Co., Ltd. Anhydrous ethanol (99.8%) was purchased from Tianjin Tianli Chemical Reagents Co. Deionized water was used during the experiments, and all chemical reagents were used without any purification.

Hydrothermal synthesis of $NaGd(MO_4)_2$:$Ho^{3+}/Tm^{3+}/Yb^{3+}$ phosphor. Preparation of RE ions $Ho^{3+}/Tm^{3+}/Yb^{3+}$-doped $NaGd(MO_4)_2$. According to the chemical formula $2Na_2MoO_4{\cdot}2H_2O + (1 - x - y - z)Gd(NO_3)_3 + xHo(NO_3)_3 + yTm(NO_3)_3 + zYb(NO_3)_3 = Na(1 - x - y - z)Gd(MO_4)_2 : xHo^{3+}/yTm^{3+}/zYb^{3+}$ was calculated and weighed for the required amount of RE oxides with a doping ratio of $NaGd(MO_4)_2$:0.1Ho/1Tm/xYb (x = 0, 10, 15, 20, and 30). The detailed test procedure is as follows. The abovementioned RE oxides were added to 10 mL of nitric acid. The excess nitric acid was evaporated while heating and stirring at a temperature of 75 °C to control pH = 7. Subsequently, the above solution was mixed with 6 mmol of Na_2MoO_4 solution, 1.25 mL of oleic acid, and 10 mL of ethanol. After stirring for 12 h, it was put into a reactor and reacted at 180° for 12 h. After natural cooling to room temperature, it was centrifuged with deionized water and absolute ethanol and dried under vacuum at 70 °C in a drying oven. After drying, the powder was taken out and placed in the Muffle furnace, heated to 800° at a heating rate of 2°/min, held for 2 h, cooled to room temperature naturally, removed, and ground for preservation.

Characterization. A DX-2700BH X-ray diffractometer (XRD), with a scanning speed of 4°/min, was used to estimate the physical structure and lattice parameters of the samples. A cold field-emission scanning electron microscope (SEM, S-4800, Hitachi) was used to characterize the microscopic morphology of the samples. A fluorescence spectrometer (FluoroLog-3, HORIBA Jobin Yvon) was used to characterize the emission spectra and pump power performance of the samples. The pump light source was a laser diode (LD) at 980 nm, and a CIE colour coordinate software analyzed the colour coordinates of the samples.

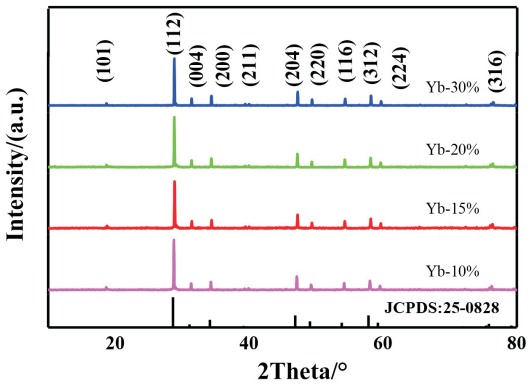


Fig. 1. XRD diagram and standard card of $Ho^{3+}/Tm^{3+}/Yb^{3+}$ doped $NaGd(MO_4)_2$ (JCPDS:25-0828)

Results and discussion. ***Measurements of XRD and SEM.*** As shown in Fig. 1, the diffraction peak exhibited by $Ho^{3+}/Tm^{3+}/Yb^{3+}$-doped $NaGd(MO_4)_2$ is consistent with that of the standard card JCPDS: 25-0828, and both have a tetragonal crystal system. Ho^{3+}, Tm^{3+}, and Yb^{3+} were used as doping ions. All these ions have the same chemical sum valence and similar ionic radii as Gd^{3+}. Thus, these ions are more likely to displace Gd^{3+} in the lattice than to form a solid solution. The cell volume of $Ho^{3+}/Tm^{3+}/Yb^{3+}$-doped $NaGd(MO_4)_2$ samples was calculated. The cell volume of pure $NaGd(MO_4)_2$in the standard card is 316.2051 $Å^3$, while those of $NaGd(MO_4)_2$: 0.1Ho/Tm/xYb (x = 0, 10, 15, 20, and 30) are 314.5270, 314.5118, 313.0613, 312.4680, and 312.1757 $Å^3$, respectively. The cell parameters for $Ho^{3+}/Tm^{3+}/Yb^{3+}$-doped $NaGd(MO_4)_2$ become smaller than pure $NaGd(MO_4)_2$due to the fact that Ho^{3+}-, Tm^{3+}-, Yb^{3+}-doped $NaGd(MO_4)_2$ replaces Gd^{3+}, leading to lattice distortions. Moreover, the radii of Ho^{3+}, Tm^{3+}, and Yb^{3+} are smaller than that of Gd^{3+} (Gd^{3+}: 0.0938 nm; Ho^{3+}: 0.0901 nm; Tm^{3+}: 0.088 nm; Yb^{3+}: 0.0868 nm), resulting in a smaller cell volume of the doped sample. No other spurious peaks appear after RE triple doping, indicating that the doping of Ho^{3+}, Tm^{3+}, and Yb^{3+} into the matrix lattice of $NaGd(MO_4)_2$ does not change the phase structure of $NaGd(MO_4)_2$. These three ions just occupy the position originally occupied by Gd^{3+}.

Figure 2a–e shows SEM images of $Ho^{3+}/Tm^{3+}/Yb^{3+}$-doped $NaGd(MO_4)_2$, i.e., for $NaGd(MO_4)_2$:0.1Ho/1Tm/xYb (x = 0, 10, 15, 20, and 30), respectively. All the particles of $NaGd(MO_4)_2$ prepared using the hydrothermal method showed a rounded spherical shape. The particle size was in the range of 0.4–0.9 μm, and all of them belong to the category of nanomaterials with slight agglomeration of grains. Moreover, the doping of $Ho^{3+}/Tm^{3+}/Yb^{3+}$ did considerably affect the particle appearance structure and grain size of $NaGd(MO_4)_2$.

UC properties. The sample of $NaGd(MO_4)_2$:$Ho^3/Tm^{3+}/Yb^{3+}$was irradiated with a 980 nm laser. Figure 3a shows the UC luminescence spectra of

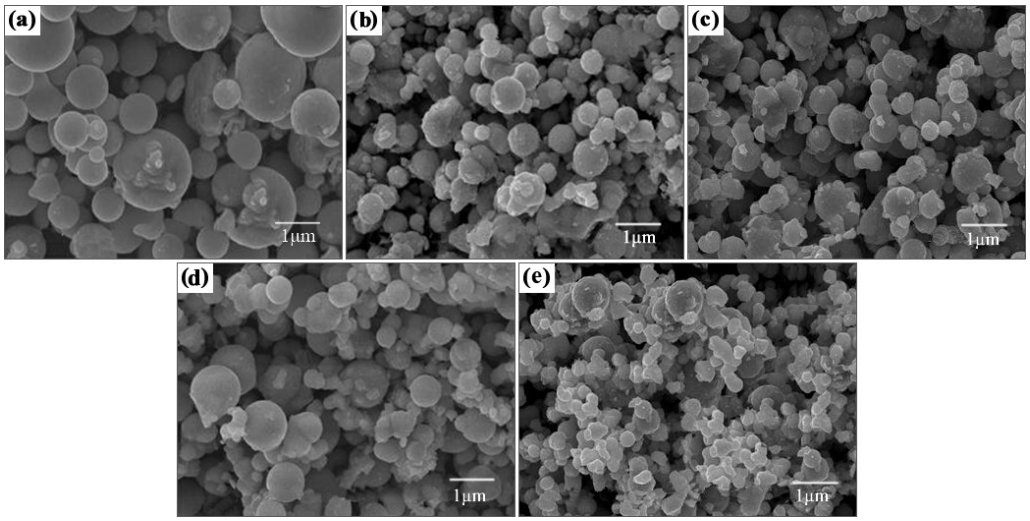


Fig. 2. SEM image of $NaGd(MO_4)_2$. **(a)** $NaGd(MO_4)_2$:0.1%Ho/1Tm/0Yb; **(b)** $NaGd(MO_4)_2$:0.1%Ho/1Tm/10Yb; **(c)** $NaGd(MO_4)_2$:0.1%Ho/1Tm/15Yb; **(d)** $NaGd(MO_4)_2$:0.1%Ho/1Tm/20Yb; **(e)** $NaGd(MO_4)_2$:0.1%Ho/1Tm/30Yb

$NaGd(MO_4)_2$:0.1Ho/Tm/xYb (x = 0, 10, 15, 20, and 30) phosphor, and the insets show the intensity variation of blue light at 477 nm, green light at 545 nm, and red light at 659 nm with Yb^{3+} doping concentration. As shown in Fig. 3a, the intensity of the blue emission peak of $NaGd(MO_4)_2$:0.1Ho/1Tm/xYb phosphor at 477 nm is greater than that of the green emission peak at 545 nm. Moreover, the intensity of the red emission peak at 659 nm is the largest, and the intensities of all three emission peaks are improved as the Yb^{3+} doping concentration increases.

As shown in Fig. 3b, the colour coordinates of $NaGd(MO_4)_2$:0.1Ho/Tm/xYb (x = 0, 10, 15, 20, and 30) as (0.5751, 0.3537), (0.4722, 0.3217), (0.3558, 0.2651), (0.3398, 0.2959), and (0.2699, 0.2555), respectively. In addition, with the increase of Yb^{3+} doping concentration, the colour coordinates of $NaGd(MO_4)_2$:0.1Ho/Tm/20Yb have gradually approached the white region, and the CIE colour coordinates of $NaGd(MO_4)_2$:0.1Ho/1Tm/20Yb are already in the white light region.

Figure 3c shows the double logarithmic curve between UC luminescence intensity and pump power for $NaGd(MO_4)_2$:0.1Ho/1Tm/20Yb phosphor. A specific function exists between the output light intensity and pump power [14]:

$$I \propto P^n,$$

where I is the UC luminescence intensity, P is the pump power, and n denotes the emission of a photon absorbed by the number of infrared photons.

To determine the value of n, the formula can be simplified to $\mathrm{Log}(I) = \mathrm{Log}(P) \times n$ using the logarithmic method, where the value of n is the slope of the

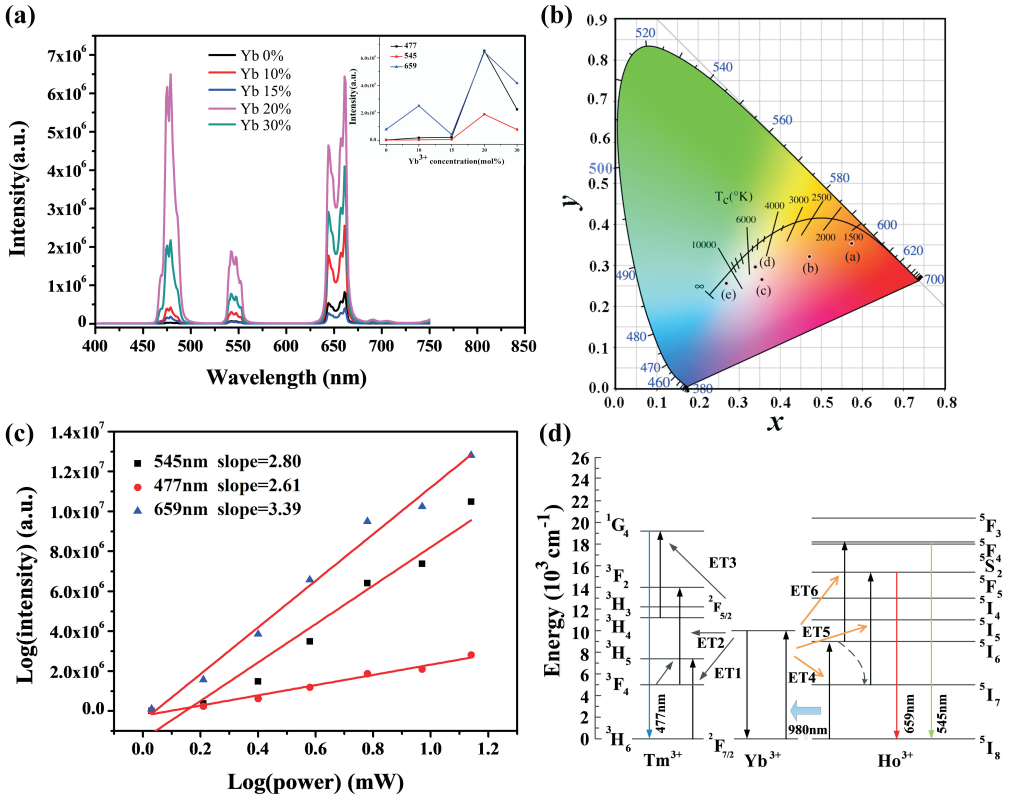


Fig. 3. The UC luminescence properties of $Ho^{3+}/Tm^{3+}/Yb^{3+}$-doped $NaGd(MO_4)_2$. **(a)** Emission spectra of $Ho^{3+}/Tm^{3+}/Yb^{3+}$-doped $NaGd(MO_4)_2$; **(b)** CIE chromatogram of $Ho^{3+}/Tm^{3+}/Yb^{3+}$-doped $NaGd(MO_4)_2$. The points a-e correspond to $NaGd(MO_4)_2$:0.1%Ho/1Tm/xYb, where x takes the values of 0, 10, 15, 20, and 30, respectively; **(c)** Luminous intensity versus pump power curve of $Ho^{3+}/Tm^{3+}/Yb^{3+}$-doped $NaGd(MO_4)_2$; **(d)** Diagram of the upconversion leap mechanism of $Ho^{3+}/Tm^{3+}/Yb^{3+}$-doped $NaGd(MO_4)_2$

fitted curve in Fig. 3. The pump power of 980 nm LD was changed to observe the change of UC luminescence intensity of $NaGd(MO_4)_2$:0.1Ho/1Tm/20Yb sample at a different power. The pump power of the laser was increased from 0.03 mW to 1.14 mW. As a result, the slope n values of the straight lines obtained by fitting at 477, 545, and 659 nm are 2.61, 2.80, and 3.39, respectively, indicating that all three types of emissions are three-photon processes.

Figure 3d shows the UC leap mechanism of $Ho^{3+}/Tm^{3+}/Yb^{3+}$-doped $NaGd(MO_4)_2$ phosphor. The analysis for deducing the UC mechanism of the $NaGd(MO_4)_2$:$Ho^{3+}/Tm^{3+}/Yb^{3+}$ phosphor shows that only Yb^{3+} can absorb the energy of 980 nm photons and transfer its absorbed energy to Ho^{3+} and Tm^{3+} through the energy transfer UC (ETU) process. First, Yb^{3+} absorbs the energy of 980 nm photons and then jumps from the ground state energy level $^2F_{7/2}$ to the excited state energy level $^2F_{7/2}$. Subsequently, it passes its energy (ET4, ET5,

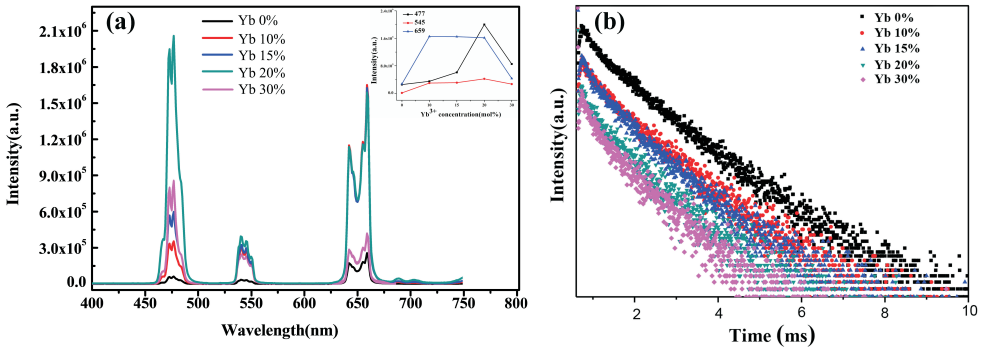


Fig. 4. Analysis of QC properties of $Ho^{3+}/Tm^{3+}/Yb^{3+}$-doped $NaGd(MO_4)_2$. **(a)** Emission spectra of $Ho^{3+}/Tm^{3+}/Yb^{3+}$-doped $NaGd(MO_4)_2$ under 446 nm excitation; **(b)** Fluorescence decay curve of $Ho^{3+}/Tm^{3+}/Yb^{3+}$-doped $NaGd(MO_4)_2$ phosphor at 545 nm

and ET6) to Ho^{3+}; hence, Ho^{3+} then jumps from the ground state energy level $^5I_8$ to the excited state energy level $^5I_6$. Furthermore, a part of Ho^{3+} will jump from the $^5I_6$ energy level to the $^5I_7$ energy level via nonradiative jump. Some of the Ho^{3+} at the $^5I_7$ energy level absorbs energy and then leaps to the $^5F_5$ energy level. Ho^{3+} at the $^5F_5$ energy level directly returns to the ground state energy level $^5I_8$ by emitting red light at 659 nm. Ho^{3+} at the $^5I_6$ energy level absorbs energy and jumps to the $(^5S_2)^5F_4$energy level, and then jumps directly to the ground state $^5I_8$energy level by emitting green light at 545 nm. Blue light emission of Tm^{3+} may be achieved by the following energy level jumping process: Yb^{3+} first absorbs the energy of 980 nm photons, corresponding to the transitions from the $^2F_{7/2}$ level to the $^2F_{5/2}$ level, and returns to the ground state through the energy transfer (ET1, ET2, and ET3) process. Tm^{3+} leaps from the ground state $^3H_6$ to the $^3H_5$ energy level, a process that requires the participation of two phonons. Tm^{3+} at the $^3H_5$ energy level then leaps nonradiatively to the $^3F_4$ energy level and subsequently leaps to the $^3F_2$ energy level through an ETU process, a process that requires the participation of three phonons. Ho^{3+} at the $^3F_2$ energy level nonradiatively leaps to the $^3H_4$ energy level and then absorbs energy to reach the $^1G_4$ energy level, from which Ho^{3+} radiolessly leaps back to the ground state $^3H_6$ by emitting 477 nm photons.

QC properties. To better characterize the QC properties of $Ho^{3+}/Tm^{3+}/Yb^{3+}$-doped $NaGd(MO_4)_2$, its emission spectra were tested under 446 nm light excitation, as shown in Fig. 4a. Figure 4b shows the fluorescence attenuation curve at 545 nm. The inset in Fig. 3a shows the variation in blue light at 477 nm, green light at 545 nm, and red light intensity at 659 nm with increasing Yb^{3+}doping concentration. When the Yb^{3+}doping concentration is $<20\%$, the peak emission intensity for red light at 659 nm becomes the highest, followed by blue light at 477 nm, and green light at 545 nm has the lowest intensity.

In the fluorescence attenuation curve test, the energy transfer efficiency η_{ET} and quantum efficiency η_{QE} were calculated according to the following formula:

$$\eta_{ET} = 1 - \frac{\tau_x}{\tau_0}, \quad \eta_{QE} = \eta_{Ho}\,(1 - \eta_{ET}) + 3\eta_{ET},$$

where η_{Ho} is the probability of radiative leap of Ho^{3+} (it is set that only the radiative leap of Ho^{3+}, Tm^{3+}, and Yb^{3+} occurs, so $\eta_{Ho} = \eta_{Yb} = 1$), τ_0 denotes the average sample lifetime of $NaGd(MO_4)_2$ when undoped with Yb^{3+}, and τ_x denotes the average lifetime of $NaGd(MO_4)_2$ doped with different Yb^{3+} concentrations.

By calculation, the average lifetime of $NaGd(MO_4)_2$ at 545 nm decreases continuously with the increase of Yb^{3+}doping concentration. The fluorescence average lifetimes of $NaGd(MO_4)_2$:0.1Ho/Tm/xYb (x = 0, 10, 15, 20, and 30) at 545 nm are 1.72, 1.51, 1.34, 1.05, and 0.96 ms, respectively. Moreover, the energy transfer efficiencies of $NaGd(MO_4)_2$:0.1Ho/Tm/xYb (x = 10, 15, 20, and 30) at 545 nm are 12.21%, 22.09%, 38.95%, and 44.19%, and the quantum efficiencies are 124.42%, 144.19%, 177.91%, and 188.37%, respectively. The average lifetime decreases continuously with the increase of Yb^{3+}doping concentration, and the energy transfer efficiency and quantum efficiency increase continuously. The energy transfer efficiency and quantum efficiency of the $NaGd(MO_4)_2$ luminescent material with 30% Yb^{3+} concentration reached the maximum value of 44.19% and 188.37%, respectively, which shows that the $Ho^{3+}/Tm^{3+}/Yb^{3+}$-doped $NaGd(MO_4)_2$ system has a high conversion efficiency under quantum shearing.

Conclusions. To sum up, the $Ho^{3+}/Tm^{3+}/Yb^{3+}$-doped $NaGd(MO_4)_2$ phosphor prepared using the hydrothermal method had a tetragonal crystal system with the morphology of blocky particles, and doping with RE $Ho^{3+}/Tm^{3+}/Yb^{3+}$ did not change the crystal structure of $NaGd(MO_4)_2$. An increase in the Yb^{3+} doping concentration considerably improved the UC performance of $NaGd(MO_4)_2$: $Ho^{3+}/Tm^{3+}/Yb^{3+}$ phosphor and all the emission peak intensities of $NaGd(MO_4)_2$: $Ho^{3+}/Tm^{3+}/Yb^{3+}$ phosphor. When Yb^{3+} concentration was 20%, the ratio of the blue light intensity of $NaGd(MO_4)_2$:0.1Ho/1Tm/20Yb at 477 nm to its red light intensity at 659 nm was gradually close to 1:1 and the colour coordinates were (0.3398, 0.2959); furthermore, the white light emission had been achieved at this doping ratio. The energy transfer and quantum efficiencies of $NaGd(MO_4)_2$:$Ho^{3+}/Tm^{3+}/Yb^{3+}$ phosphors were continuously increased with increasing Yb^{3+} concentration. The energy transfer and quantum efficiencies of $NaGd(MO_4)_2$: 0.1Ho /Tm/30Yb could reach 44.19% and 188.37%, respectively. These results demonstrate the efficient energy transfer and superior quantum clipping properties of $NaGd(MO_4)_2$: $Ho^{3+}/Tm^{3+}/Yb^{3+}$ with potential applications in white light illumination and the improvement of LED illumination efficiency.

REFERENCES

[1] Lyu L., H. Cheong, X. Ai, W. Zhang, J. Li et al. (2018) Near-infrared light-mediated rare-earth nanocrystals: recent advances in improving photon conversion and alleviating the thermal effect, NPG Asia Materials, **10**(8), 685–702.

[2] Wilhelm S. (2017) Perspectives for upconverting nanoparticles, ACS nano, **11**(11), 10644–10653.

[3] Kumar A., M. Kumar, V. Bhatt, D. Kim, S. Mukherjee et al. (2021) ZnS microspheres-based photoconductor for UV light-sensing applications, Chemical Physics Letters, **763**, 138162.

[4] Yang C., J. Zhang, W.-T. Peng, W. Sheng, D. Liu et al. (2018) Impact of Stokes Shift on the Performance of Near-Infrared Harvesting Transparent Luminescent Solar Concentrators, Scientific Reports, **8**(1), 16359.

[5] Pandey A., R. Vineet Kumar, R. Dey, K. Kumar (2013) Enriched green upconversion emission in combustion synthesized Y_2O_3:Ho^{3+}, Yb^{3+} phosphor, Materials Chemistry and Physics, **139**(2–3), 483–488.

[6] Tian Y., B. Li, J. Wang, Q. Liu, Y. Chen et al. (2019) The mid-infrared emission properties and energy transfer of Tm^{3+}/Er^{3+} co-doped tellurite glass pumped by 808/980 nm laser diodes, Journal of Luminescence, **214**(11), 116586.

[7] Fan X., J. Nie, W. Ying et al. (2021) Cryogenic enabled multicolor upconversion luminescence of $KLa(MoO_4)_2$:Yb^{3+}/Ho^{3+} for dual-mode anti-counterfeiting, Dalton Transactions, **50**(35), 12234–12241.

[8] Zou Z., T. Wu, H. Lu et al. (2018) Structure, luminescence and temperature sensing in rare earth doped glass ceramics containing $NaY(WO_4)_2$ nanocrystals, RSC advances, **8**(14), 7679–7686.

[9] Gao X., J. Yang, M. Zhang et al. (2019) Preparation and optical properties of Eu^{2+} doped $12CaO{\cdot}7Al_2O_3$ blue emitting conductive phosphors, Chinese Journal of Luminescence, **40**(7), 849–856.

[10] Klier D., M. Kumke (2015) Upconversion luminescence properties of $NaYF_4$:Yb:Er Nanoparticles Codoped with Gd^{3+}, Journal of Physical Chemistry C, **119**(6), 3363–3373.

[11] Li Y., S. Zhou, G. Dong et al. (2014) Anti-Stokes Fluorescent Probe with Incoherent Excitation, Scientific Reports, **4**(1), 4059.

[12] Shi Z., J. Wang, X. Guan (2018) Preparation and upconversion luminescence properties of $Nd^{3+}/Yb^{3+}/Tm^{3+}$ Co-doped $NaY(WO_4)_2$ nanocrystals, Journal of the Chinese Ceramic Society, **46**(1), 136–141.

[13] Nadort A., J. Zhao, E. Goldys (2016) Lanthanide upconversion luminescence at the nanoscale: fundamentals and optical properties, Nanoscale, **8**(27), 13099–13130.

[14] Xu H., K. Xu, A. Lu (2015) Microwave hydrothermal synthesis and white upconversion emission of NaGd $(WO_4)_2$:($Yb^{3+}/Tm^{3+}/Ho^{3+}$) phosphors, Journal of Materials Science: Materials in Electronics, **26**, 3921–3925.

School of Materials Science and Engineering
Chang'an University, Xi'an 710061, China
e-mails: zzg202307@163.com, 610372498@qq.com, 2312666016@qq.com, 1483501778@qq.com, 2456331408@qq.com